Automotive Science and Engineering, Vol. 12, No. 4, (2022), 3960-3970

Iran University of Science and Technology

Automotive Science and Engineering

Journal Homepage: ase.iust.ac.ir

ISSN: 2008-9899

Performance of Absorptive Material Liners on Noise Transmission Loss in Mufflers used by Goods Carrying Tricycles

Eric Amoah Asante[1]*, Randy Amuaku[2]

[1]Department of Agricultural and Biosystems Engineering, College of Engineering, Kwame Nkrumah University of Science and Technology, Kumasi, Ghana

[2]Department of Mechanical Engineering, Faculty of Engineering, Koforidua Technical University, Koforidua, Ghana

ARTICLE INFO

Article history:
Received: 12 Aug 2022
Accepted: 10 Sep 2022
Published:2 Oct 2022

Keywords:
Tricycle,
PLSR,
Transmission Loss,
Absorptive Material Liner

A B S T R A C T

Due to the increase in the number of goods carrying tricycles, the amount of noise and pollution on our roads has increased. Different absorptive material liners have been introduced into muffler design to optimize the control of the engine noise emission for tricycles. In this study, the performance of Aerogel, Ceramic, Kenaf fibre, Polyester and Rockwool as absorptive material liners on the transmission loss under 20 ℃, 60 ℃, 100 ℃, 150 ℃ and 200 ℃ temperature treatment for goods carrying tricycle was evaluated. The analysis averaged over all temperature treatments showed that introducing absorptive materials into the muffler improved the performance by 71.56 %, 84.12 %, 86.31 %, 89.37 % and 93.99 % for Aerogel, Rockwool, Ceramic, Polyester and Kenaf fibre respectively. Similarly, analysis averaged over all absorptive material treatments disclosed that the muffler with an absorptive material liner under 60 ℃, 100 ℃, 150 ℃ and 200 ℃ temperature treatment improved the performance over the muffler without a liner by 85.1 %, 80.8 %, 87.5 % and 92.3 % respectively. The flow resistivity values for the absorptive material liners used were inversely proportional to the transmission loss except for the Kenaf fibre which had the highest transmission loss though with the second highest flow resistivity. PLSR analysis showed that Aerogel, Rockwool, Ceramic, Polyester and Kenaf fibre yielded better prediction accuracy than the No liner by 33.88%, 32.75%, 30.45%, 30.41% and 22.35% respectively. The study has confirmed that introducing absorptive material liners in mufflers used by goods carrying tricycles can optimize performance.

1. Introduction

Tricycles are widely used in most parts of Africa and the world as a whole for carrying waste materials, heavy metals, raw materials and also for conveying goods to places such as markets, storage centres (silos), and factories [1, 2]. They are very efficient and makes the transportation of goods very easy. However, they produce a lot of noise during operation. The amount of noise generated by the engine through the exhaust system is ten times more than the structural noise [3]. The noise produced by engines during combustion has effects on hearing in humans. Mufflers play important role in noise control during transmission by reducing emitted noise flowing through the exhaust of an internal combustion engine. Noise Transmission loss is the ratio of the sound power of the incident (progressive) pressure wave at the inlet of the muffler to the sound power of the transmitted

*Corresponding Author
Email Address: ericasante@knust.edu.gh
http://doi.org/10.22068/ase.2022.598

[DOI: 10.22068/ase.2022.598]

pressure wave at the outlet of the muffler. Research over a decade has shown that different geometric features have been introduced into the muffler design concepts to achieve optimum noise transmission loss characteristics [4]. Some of the geometrical parameters introduced include the expansion of resonator chambers, an extension of input and output tubes, resonator chamber perforation and the use of absorptive material liners or filters. These absorptive material liners when used absorb the sound waves propagating from the exhaust system. Absorptive material liners such as Basalt and resonated cotton have been known and produced commercially for acoustic treatment [5]. In acoustic treatments, fabric-like materials are efficient acoustic absorbers, but in terms of vibration they are usually framed in rigid structures or sandwiched layers [6]. The absorptive material liners play an important role in the performance of the muffler because of certain embedded mechanical properties. Research conducted by [7, 8] show that several porous or fibrous absorptive materials can be used for noise reduction in the exhaust system during combustion. Their results also show that materials have absorption properties depending upon frequency, composition, liner thickness, airflow resistivity, mean fibre diameter, temperature, surface finish and method of application. There are several methods of predicting the performance of a muffler, however, Finite Element Method (FEM) is widely used and relevant literature can be found regarding the acoustic modelling of mufflers. With the evolution of different simulation software, the use of FEM is becoming easier. Literature review shows that several researchers have used absorptive material liners under FEM analysis to predict the noise transmission loss of mufflers. For instance [9], predicted the transmission loss of an exhaust system using polyester liner as an absorptive material. Also, [10] used Rockwool as an absorptive material liner with the aid of finite element method approach to predict transmission loss characteristics for different parameter combination of a muffler under a 4-pole system. In another study, [11] predicted the transmission loss characteristics in a coupled hybrid muffler using FEM. Similarly, [12] investigated the effects of absorptive material, the porosity of baffle plates, and perforated tubes on the acoustic attenuation performance of a three-chamber U-bend hybrid muffler by 1D transfer matrix method and 3D FEM. Based on the findings, design guidelines were developed for these types of muffler configurations in order to improve their performance. In recent years, many studies have shown the use of absorptive material liners and metamaterials combined to reduce noise levels in mufflers through experiment and FEM. For instance, [13, 14] demonstrated the effectiveness of acoustic metamaterial structures with honeycomb and square unit cell in sound control applications, in comparison with conventional sound barriers. This design was further tuned to achieve an acoustic stop band gap at a chosen frequency band in a muffler with acoustic metamaterials in order to affect the transmission loss [15].

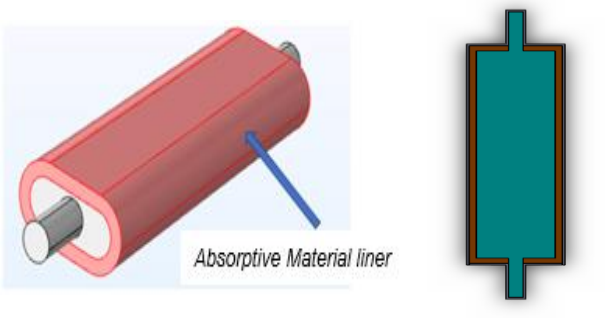

(a) (b)

Figure 1*: Schematic diagram of (a) Muffler with an external liner, (b), Sectional view of the muffler with internal liner*

Based on the literature reviewed, it is now clear that the introduction of absorptive material liners on a muffler has a significant effect on performance optimization. Therefore, this study seeks to: (1) evaluate the performance characteristics of absorptive material liners on goods carrying tricycle mufflers, (2) predict the optimum absorptive material liner for mufflers of goods carrying tricycle based on temperature variations, flow resistivity, and mean fiber diameter parameters using Comsol Multiphysics Software, (3) predict an optimum absorptive material liner for goods carrying tricycle mufflers through computational fluid dynamics (CFD) using ANSYS Fluent software and (4) predict the positioning of absorptive material liner on goods

[DOI: 10.22068/ase.2022.598]

carrying tricycle mufflers for optimum noise transmission loss characteristics.

2. Materials, Model Description and Methods

2.1 Theoretical Model Analysis in Comsol Multiphysics

Absorptive mufflers use the principle of absorption to reduce sound energy [16]. The propagation of sound waves is reduced when the energy is converted into heat by the absorptive material liners. A typical absorptive muffler consists of a hollow circular pipe which is straight and enclosed with shell layers [17]. In this study, the proposed muffler model comprises of two hollow pipes attached to an elliptical casing at both ends, that serves as input and output ends for the wave propagation. The casing accommodates the material liner that absorbs the sound pressure pulses during transmission. The mathematical computations that explain the propagation of sound in the fluid type medium can be calculated from the fluid flow equations [18]. In most acoustic cases, the fluid flow losses and viscous effects are neglected leading to the use of a linearized equation of state. Based on this assumption, the acoustic field which is described as pressure is governed by the wave equation as;

$$\frac{1}{\rho_o c^2}\frac{\partial^2 p}{\partial t^2}+\nabla.\left[-\frac{1}{\rho_o}(\nabla p-q)\right]=Q \qquad (1)$$

Where ρ_o is the density of the fluid in (kg/m^3), t is the time in seconds, q and Q are the expected acoustic sources (N/m^3). The model equation can further be simplified into a modified version of the Helmholtz equation for the acoustic pressure p in the muffler as:

$$\nabla.\left(-\frac{\nabla p}{\rho}\right)-\frac{\omega^2 p}{c^2\rho}=0 \qquad (2)$$

Where, ρ is the density, c is the speed of sound and, ω is the angular frequency. For porous absorptive material liners with a rigid skeleton, a well-known model is used to estimate its parameters such as frequency and flow resistivity. The Delany-Bazley model is a simple and fast approximation technique for the estimation of acoustic isotropic layer parameters with homogenous porous absorptive material liner [19]. The acoustic parameters such as characteristic impedance (Z_c), the propagation constant k_c and surface acoustic impedance (Z) can be computed as:

$$\begin{aligned} k_c &= k_a\left(1+0.098\cdot\left(\frac{\rho_a f}{R_f}\right)^{-0.7}-i\cdot 0.189\cdot\left(\frac{\rho_a f}{R_f}\right)^{-0.595}\right) \\ z_c &= z_a\left(1+0.057\cdot\left(\frac{\rho_a f}{R_f}\right)^{0.734}-i\cdot 0.087\cdot\left(\frac{\rho_a f}{R_f}\right)^{-0.732}\right) \end{aligned} \qquad (3)$$

Where, R_f is the flow resistivity, $k_a=\omega/c_a$ and $z_a=\rho_a/c_a$ are the free space wavenumber and impedance of air respectively. The flow resistivity for glass wool-like materials was determined based on the Bies and Henson definition as follows [20];

$$R_f=\frac{3.18\cdot 10^{-19}\cdot\rho^{1.53}}{d_{av}{}^2} \qquad (4)$$

Where, d_{av} is the mean fibre diameter of the absorptive material liners; An important parameter of an absorptive muffler is the transmission loss or attenuation. The transmission loss characteristic of the absorptive muffler is the ratio of incoming acoustic energy to outgoing acoustic energy as:

$$TL=10\log\left(\frac{\omega_{in}}{\omega_{out}}\right) \qquad (5)$$

Where, TL is the transmission loss characteristics, ω_{in} is the incoming acoustic energy and ω_{out} is the outgoing acoustic energy. The incoming acoustic energy (ω_{in}) and outgoing acoustic energy (ω_{out}) can be calculated as;

$$\omega_{in}=\int_{\partial\Omega}\frac{|p|^2}{2\rho c}dA;\ \omega_{out}=\int_{\partial\Omega}\frac{p_o{}^2}{2\rho c}dA \qquad (6)$$

The finite element method (FEM) was performed in the acoustic module of comsol multiphysics software. Since the absorptive material liners are porous, Delany and Bazley's equations were used to determine the complex wavenumber k_c and complex impedance z_c of the liners which estimate the acoustic parameters as a function of frequency and airflow resistivity [21].

2.2 Turbulence Modelling in ANSYS-Fluent

[DOI: 10.22068/ase.2022.598]

In this paper, $K-\varepsilon$ method is used for turbulence modeling. ANSYS-fluent software has several turbulence models by default. In general, there are two methods of averaging Reynolds and filtering to replace the solving of Navier–Stokes equations in turbulent flows. Navier-stokes equations, averaged by the Reynolds method govern the transfer of averaged quantities [22]. Both methods model the entire range of amplitude scales for the turbulent flow. The $K-\varepsilon$ is a two-equation model which contains two additional transitional equations and was used to calculate the properties of turbulence flow as shown in equation (7). In this model, the turbulent flow field is defined in two variables; K determines the energy in turbulence and ε determines the scale of turbulence

$$K=\frac{1}{2}\overline{u_i' u_i'},\ \varepsilon=(\frac{\mu}{\rho})\overline{u_{i,J}' u_{i,J}'} \tag{7}$$

Using dimensional analysis, turbulent viscosity μ_t can be related to the length of the large Eddy-scale turbulent flow as:

$$\mu_t \alpha \rho u_i \delta_l \tag{8}$$

Where u_l is the velocity of the scale and δ_l is the length of the large Eddy-scale turbulent flow. Therefore, it can be shown as:

$$u_l \alpha \sqrt{k}$$
$$\delta_l \alpha \frac{\sqrt{k^3}}{\varepsilon} \tag{9}$$

By substituting equations (9) into equation (8), the following equation is obtained.

$$\mu_t = C_\mu \rho \frac{k^2}{\varepsilon} \tag{10}$$

Where C_μ is the experimental coefficient which is usually considered 0.09. In the standard $K-\varepsilon$ model, the values K and ε are obtained by the following quasi-experimental equations;

Where C_1, C_2 and C_3 are experimental coefficients, σ_ε is the turbulent Schmidt number and σ_k is the turbulent Prandtl number. $C_1\left(\frac{\varepsilon}{k}\right)G$ and $C_2\rho\left(\frac{\varepsilon^2}{k}\right)$ in equation (7) represent the shear generation processes and the viscous dissolution processes respectively.

$C_1(1-C_3)\frac{\varepsilon}{k}B$ represents Buoyancy effects. In

$$\begin{cases}\rho\frac{\partial k}{\partial t}+\rho u_j k_j=\left(\mu+\frac{\mu_t}{\sigma_k}k_j\right)_j+G+B-\rho\varepsilon\\ \rho\frac{\partial \varepsilon}{\partial t}+\rho u_j \varepsilon_{,j}=\left(\mu+\frac{\mu_t}{\sigma_\varepsilon}\varepsilon_{,j}\right)_j+C_1\frac{\varepsilon}{k}G+C_1(1-C_3)\frac{\varepsilon}{k}B-C_2\rho\frac{\varepsilon^2}{k}\end{cases} \tag{11}$$

equation (11), G is the amount of the turbulent kinetic energy produced by the interaction between the mean flow and the turbulent flow field.

Therefore, it is called shear generation. The B also indicates the generation of the Buoyancy loss. The exact relations for G and B are as follows:

$$G=-\rho\overline{u_i' u_j' u_{i,j}},\ B=\overline{\rho' u_i' g_i} \tag{12}$$

The basic relation of Boussinesq is based on the principle that the Reynolds stress components are proportional to the average velocity gradients as shown in the following equation.

$$-\rho\overline{u_i' u_j'}=2\mu_t S_{ij}-\frac{2}{3}\rho k\delta_{ij} \tag{13}$$

Where S_{ij} is the average strain-rate tensor and is defined by the formula;

$$S_{ij}=\frac{1}{2}\left(\frac{\partial u_j}{\partial x_i}+\frac{\partial u_i}{\partial x_j}\right) \tag{14}$$

By substituting the basic relation of Boussinesq (12) in equation (13), the following equation can be obtained:

$$G\approx\mu_t\left(u_i u_j+u_{j,i}\right)u_{i,j},\ B\approx-\frac{\mu_t}{\rho\sigma_P}\rho_i g_i \tag{15}$$

Input parameters of the fluid for computational fluid dynamics (CFD) simulation has been provided in Table 1.

Table 1. *Input parameters of the fluid*

Parameters	*Value*
Fluid	*Air (ideal gas)*
Speed of sound, c	*343 m/s*
Density, ρ	*1,2041 kg/m^3*
Inlet velocity, u	*10 m/s*

Input parameters of the acoustic medium in Comsol Multiphysics are provided in Table 2,

[DOI: 10.22068/ase.2022.598]

Table 2. *Input parameters of acoustic medium*

Parameters	***Value***
Fluid	*Air (ideal gas)*
Speed of sound	$343\ m/s$
Atmospheric pressure (P_O)	*1.0133E5 Pa*
Inlet pressure (P_{in})	*1 P_a*
Temperature	*20,60,100,150,200[°C]*

The muffler models were developed in 3D as shown in Figure 1. Subsequently, different boundary conditions were applied. The boundary conditions include (1) The outer wall which is the solid boundary of the chamber and tubes, sound hard (wall) boundary condition was applied with a normal velocity of zero. (2) At the inlet boundary, incoming and outgoing plane waves exist. Therefore, the inlet pressure was taken as 1Pa. (3) At the outlet boundary, the radiation condition was applied for outgoing plane waves. (4) The photoacoustic boundary condition was applied to the muffler. The absorptive material liner properties including flow resistivity, mean fiber diameter, and density were inserted into the subdomain condition. The model meshed and a frequency domain study was applied. The analysis was performed within a frequency range of $0Hz \sim 3000\,\mathrm{Hz}$. The solution yielded varying acoustic pressure and sound pressure level transmission in the inner section of the absorptive muffler within the frequency range. Subsequently, the transmission loss characteristics of the muffler were calculated. To achieve the objectives of this research several absorptive material liners were considered. The materials were selected based on the literature available on the design and evaluation of absorptive mufflers. The properties of the absorptive material used are presented in Table 3,

Table 3. *Absorptive Material Parameters*

Material	***Flow Resistivity [N*s*m^{-4}]***	***Poisson Ratio (v)***	***Young Modulus (MPa) / N/m^2***	***Density kg/m^3***	***Mean Fibre Diameter [m]***
Kenaf fibre	*30063.77*	*0.324*	*708*	*83.75*	*0.0769*
Polyester	*5356*	*-0.75*	*920*	*44.00*	*0.032*
Aerogel	*9.93e10*	*0.24*	*10^7*	*1.24*	*0.0403*
Rockwool	*11817.5*	*0.21*	*72*	*62.20*	*0.050*
Ceramic fibre	*6060*	*0.37*	*288*	*68.00*	*0.055*

2.3 Statistical evaluation of model performance

Statistical method such as partial least square regression (PLSR) was used to obtain information on the performance of the absorptive material liner. PLSR can simply treat data matrices in which each item is described by hundreds of variables like Transmission loss data [23]. This technique can extract the relevant portion of the information for large data matrix and produce the most dependable models. The correlation coefficient (R) of the prediction set (R_p) and the root mean square error of the prediction set (RMSEP) are used to evaluate prediction precision. R_p measures the degree of correlation between the predicted and simulated values. It is computed by the following expression;

$$R = \frac{\sum_{i=1}^{N}(T_{is} - \bar{T}_{is})(S_{ip} - \bar{S}_{ip})}{\sqrt{\sum_{i=1}^{N}(T_{is} - \bar{T}_{is})} * \sqrt{\sum_{i=1}^{N}(S_{ip} - \bar{S}_{ip})}} \quad (16)$$

Where T_{is} and $\bar{T}_{is}$ are the reference values of the i^{th} sample and the average values of the reference values respectively; S_{ip} and $\bar{S}_{ip}$ are the predicted values of the i^{th} and the average values of the predicted values respectively; N is the number of the samples. The RMSE of the predicted values S_{ip} for observations i of a regression's dependent variable T_{is} is computed for N different predictions as the square root of the mean of the squares of the deviations. It is given by:

$$RMSE = \sqrt{\frac{\sum_{i=1}^{N}(S_{ip} - T_{is})^2}{N}} \quad (17)$$

3. Results and Discussion

3.1 Noise Transmission Loss Analysis

In the simulation of the muffler, certain absorptive material liner parameter computations were considered. In the first condition, a standard

[DOI: 10.22068/ase.2022.598]

muffler without absorptive material liner was studied. Subsequently, five absorptive material liners were introduced into the muffler model and analyzed at varying temperatures. The noise transmission loss characteristics for the various absorptive material liners was calculated at varying temperatures of 20℃,60℃,100℃,150℃, 200℃ and the results compared to the muffler without any absorptive material liner (Figure 2). The trend showed an obvious rise to major peaks at different frequencies for all the absorptive material liners except for the Aerogel and the No liner where several peaks occurred along the transmission path. Furthermore, the number of transmission peaks reduces with increasing transmission loss. The higher the flow resistivity value, the higher the output and the lower the input to output ratio leading to a lower transmission loss. This trend is established in Figure 2 (a, b and d) except the Kenaf fibre which had the highest transmission loss though with a second highest flow resistivity value which could be due to thermal conductivity and other material properties [24, 25].

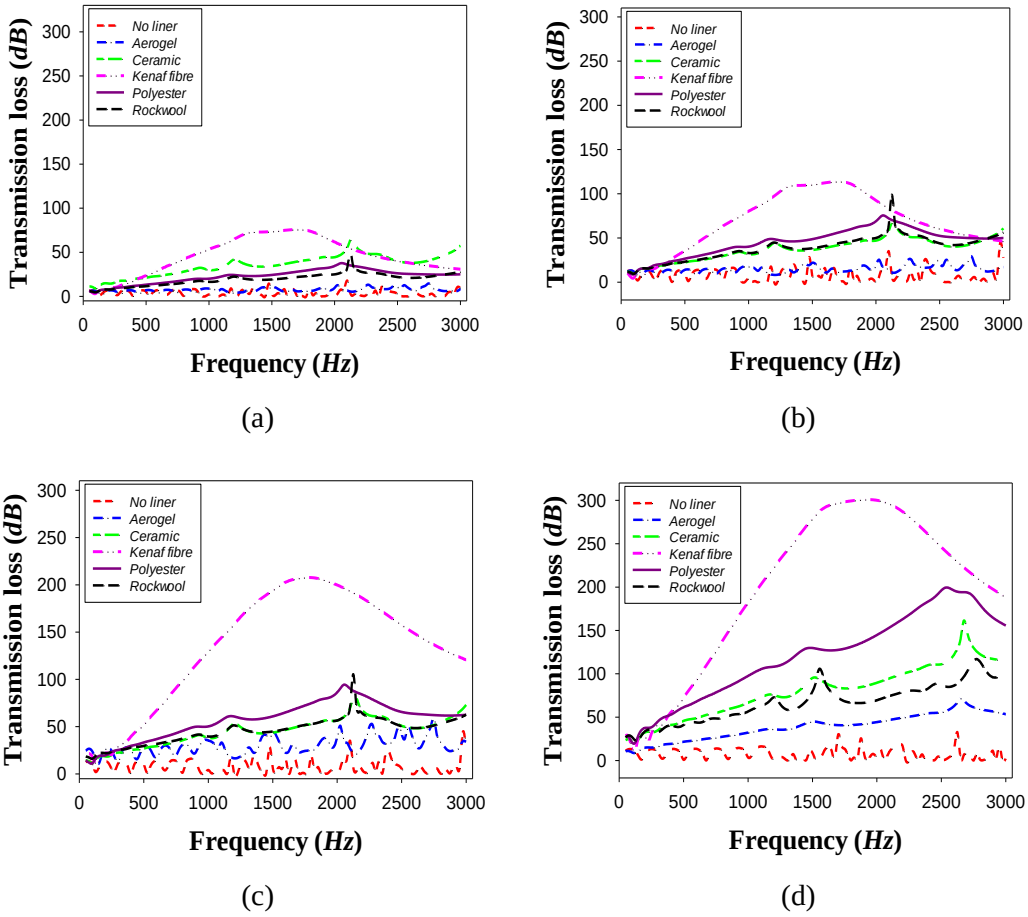

Figure ۲. *Noise Transmission loss at a temperature of (a) 60℃ (b)100℃, (c)150℃ (d)200℃*

It was difficult to evaluate the results qualitatively due to the overlaps and crossovers. Therefore, quantitative analysis was employed to determine the differences. The quantitative analysis averaged over all temperature treatments showed that, introducing absorptive material liners into the muffler improved the performance by 71.56%, 84.12%, 86.31%, 89.37% and 93.99% for Aerogel, Rockwool, Ceramic, Polyester and Kenaf fibre respectively. Similarly, quantitative analysis averaged over all absorptive material treatments disclosed that, the muffler with material liner under 60℃, 100℃, 150℃ and 200℃ temperature treatments improved the performance over the muffler without a liner by 85.1%, 80.8%, 87.5% and 92.3% respectively. The initial higher value of the 60℃ treatment was due to a very low response value for the No liner muffler which resulted into a bigger difference. Table 4 presents the results for the transmission loss (dB) at varied frequency range under different temperatures for the various absorptive material liners.

***Table 4**, Transmission loss at varying Temperatures*

[DOI: 10.22068/ase.2022.598]

Absorptive Material Liner	*Temp 60 ℃*	*Temp 100 ℃*	*Temp 150 ℃*	*Temp 200 ℃*
	TL (dB)	*TL (dB)*	*TL (dB)*	*TL (dB)*
Frequency Range (Hz)	*(0~1000)*	*(0~1000)*	*(0~1000)*	*(0~1000)*
No Liner	*7.41*	*14.59*	*16.34*	*14.59*
Aerogel	*9.04*	*18.09*	*36.19*	*32.18*
Ceramic	*32.42*	*32.63*	*40.65*	*66.64*
Kenaf fibre	*53.52*	*80.28*	*80.28*	*182.38*
Polyester	*20.01*	*40.02*	*50.22*	*97.56*
Rockwool	*17.59*	*35.19*	*35.19*	*56.50*
Maximum Transmission Loss (TL) at Frequency Range (0~1000) Hz	*53.52 (1000) Hz*	*80.28 (975) Hz*	*80.28 (1000) Hz*	*182.38 (1000) Hz*
Frequency Range (Hz)	*(1000~2000)*	*(1000~2000)*	*(1000~2000)*	*(1000~2000)*
No Liner	*9.98*	*28.48*	*28.42*	*29.98*
Aerogel	*11.01*	*22.02*	*44.05*	*44.98*
Ceramic	*44.63*	*47.03*	*56.67*	*95.73*
Kenaf fibre	*75.78*	*113.74*	*113.59*	*300.93*
Polyester	*34.47*	*68.95*	*86.19*	*144.77*
Rockwool	*25.00*	*49.62*	*49.62*	*105.03*
Maximum Transmission Loss (TL) at Frequency Range (1000~2000) Hz	*75.78 (1725) Hz*	*113.74 (1700) Hz*	*113.59 (1675) Hz*	*300.93 (1925) Hz*
Frequency Range (Hz)	*(2000~3000)*	*(2000~3000)*	*(2000~3000)*	*(2000~3000)*
No Liner	*18.03*	*43.28*	*44.28*	*32.72*
Aerogel	*12.99*	*29.26*	*58.52*	*71.66*
Ceramic	*63.70*	*60.84*	*73.01*	*161.44*
Kenaf fibre	*60.04*	*90.07*	*90.07*	*299.43*
Polyester	*37.69*	*75.39*	*94.24*	*199.03*
Rockwool	*49.46*	*50.00*	*98.93*	*116.96*
Maximum Transmission Loss (TL) at Frequency Range (2000~3000) Hz	*63.70 (2125) Hz*	*90.07 (2025) Hz*	*98.93 (2125) Hz*	*299.43 (2025) Hz*

3.1.1 Computational Fluid Dynamics (CFD) Analysis

To show the practical application of the proposed model with the existence of the absorptive material liners, the fluid dynamics and pressure drop characteristics of the models were simulated in this section. For CFD analysis the fluid which is modeled is an ideal gas and the flow inlet velocity is fixed at 10 m/s, gas temperature is assumed to change from 20~200℃. The results of the CFD simulations are shown in table 5. Moreover, contour plots of a velocity, pressure and temperature of the muffler with different absorptive material liners obtained-see Appendix for the details. The results in Table 5, indicated that the pressure and velocity are inversely proportional to each other. Bernoulli's principle states that as the velocity increases, the pressure decreases to keep the algebraic sum of the potential energy, kinetic energy and pressure constant.

Table 5. *Results of CFD simulation*

Muffler with the existence of Polyester												
Temperature	*۲۰ ℃*		*60 ℃*		*80 ℃*		*100℃*		*150℃*		*200℃*	
	inlet	*outlet*	*inlet*	*outlet*	*inlet*	*outlet*	*inlet*	*outlet*	*inlet*	*outlet*	*inlet*	*outlet*
Velocity (m/s)	*10*	*10.18*	*10*	*10.14*	*10*	*10.14*	*10*	*10.14*	*10*	*10.14*	*10*	*10.14*
Pressure (Pa)	*91.19*	*0.11*	*119.46*	*1.88*	*119.52*	*2.69*	*119.67*	*1.30*	*119.67*	*1.89*	*119.58*	*2.96*
Temperature(K)	*293.15*	*293.15*	*333.15*	*333.14*	*353.15*	*353.15*	*373.15*	*373.14*	*423.15*	*423.15*	*473.15*	*473.15*
Muffler with the existence of Aerogel												
Temperature	*۲۰ ℃*		*60℃*		*80℃*		*100℃*		*150℃*		*200℃*	
	inlet	*outlet*	*inlet*	*outlet*	*inlet*	*outlet*	*inlet*	*outlet*	*inlet*	*outlet*	*inlet*	*outlet*
Velocity (m/s)	*10*	*10.35*	*10*	*10.40*	*10*	*10.58*	*10*	*10.58*	*10*	*10.58*	*10*	*10.61*
Pressure (Pa)	*143.57*	*2.75*	*145.85*	*2.81*	*145.89*	*2.89*	*148.89*	*2.89*	*148.88*	*2.89*	*149.01*	*2.89*
Temperature(K)	*293.15*	*293.15*	*333.15*	*333.14*	*353.15*	*353.15*	*373.15*	*373.15*	*423.15*	*423.15*	*473.15*	*73.16*
Muffler with the existence of Rockwool												
Temperature	*۲۰℃*		*60 ℃*		*80 ℃*		*100 ℃*		*150 ℃*		*200 ℃*	

[DOI: 10.22068/ase.2022.598]

	inlet	*outlet*	*inlet*	*outlet*	*inlet*	*outlet*	*inlet*	*outlet*	*inlet*	*outlet*	*inlet*	*outlet*
Velocity (m/s)	*10*	*10.79*	*10*	*10.79*	*10*	*10.80*	*10*	*10.80*	*10*	*10.80*	*10*	*10.80*
Pressure (Pa)	*132.12*	*2.01*	*143.79*	*2.10*	*143.57*	*2.19*	*143.72*	*2.20*	*143.68*	*2.20*	*143.69*	*2.21*
Temperature(K)	*293.15*	*293.15*	*333.15*	*333.14*	*353.15*	*353.14*	*373.15*	*373.14*	*423.15*	*423.15*	*473.15*	*473.14*
Muffler with the existence of Ceramic												
Temperature	*٢٠℃*		*60 ℃*		*80 ℃*		*100 ℃*		*150 ℃*		*200 ℃*	
	inlet	*outlet*	*inlet*	*outlet*	*inlet*	*outlet*	*inlet*	*outlet*	*inlet*	*outlet*	*inlet*	*outlet*
Velocity (m/s)	*10*	*10.16*	*10*	*10.17*	*10*	*10.17*	*10*	*10.17*	*10*	*10.17*	*10*	*10.12*
Pressure (Pa)	*86.16*	*1.12*	*45.58*	*0.04*	*45.59*	*0.08*	*45.60*	*0.08*	*45.65*	*0.08*	*45.66*	*0.10*
Temperature(K)	*293.15*	*293.15*	*333.15*	*333.15*	*353.15*	*353.15*	*373.15*	*373.15*	*423.15*	*423.15*	*473.15*	*473.15*
Muffler with the existence of Kenaf fibre												
Temperature	*٢٠℃*		*60 ℃*		*80 ℃*		*100 ℃*		*150 ℃*		*200 ℃*	
	inlet	*outlet*	*inlet*	*outlet*	*inlet*	*outlet*	*inlet*	*outlet*	*inlet*	*outlet*	*inlet*	*outlet*
Velocity (m/s)	*10*	*10.14*	*10*	*10.14*	*10*	*10.14*	*10*	*10.14*	*10*	*10.14*	*10*	*10.14*
Pressure (Pa)	*119.41*	*1.30*	*119.61*	*1.33*	*119.40*	*1.41*	*119.54*	*2.76*	*119.70*	*2.98*	*119.71*	*3.01*
Temperature(K)	*293.15*	*293.14*	*333.15*	*333.14*	*353.15*	*353.14*	*373.15*	*373.14*	*423.15*	*423.14*	*473.15*	*473.14*

3.2 Effects of Absorptive material liner on prediction accuracy

In order to validate the effect of absorptive material liner on the model, PLSR was used to predict the transmission loss within a frequency range of 0~3000 Hz. The scatter plots for the correlation between the simulated values and the predicted values as influenced by the temperature differences are presented in Figure 3. Detailed information on R^2 and RMSE values are calculated through the regression between the simulated and predicted liner material variables (Table 6). In this study, two indices were employed to compare and validate the effect of absorptive material liner on the performance of the models. It was because R^2 and RMSE are the most useful and commonly used indices for evaluating the performance of models [26].

Table 6*. Results of statistical PLSR modeling*

Absorptive Material Liners	***Correlation Coefficient (R^2)***	***RMSE***
Aerogel	*0.8881*	*0.1010*
Rockwool	*0.8732*	*0.1317*
Ceramic	*0.8443*	*0.1541*
Polyester	*0.8438*	*0.1708*
Kenaf fibres	*0.7562*	*0.2507*
No Liner	*0.5820*	*0.0787*

Evaluating the performance of the models (Table 6) showed that *Aerogel* (R^2 *= 0.881, RMSE = 0.1010*) > *Rockwool* (R^2 = 0.8732, *RMSE = 0.1317)* > *Ceramic* (R^2 *= 0.8443, RMSE= 0.1541)* > *Polyester* (R^2 *= 0.8438, RMSE = 0.1708)* > *Kenaf fibre* (R^2 *= 0.762, RMSE = 0.2507)* > *No liner* (R^2 *= 0.5820, RMSE = 0.0787).* Subsequently, the performance of the model shows that the higher the peak, the lower the prediction accuracy for a given absorptive material liner. Furthermore, the models showed that the Aerogel, Rockwool, Ceramic, Polyester and Kenaf fibre yielded a better prediction accuracy than the No liner by 33.88 %, 32.75 %, 30.45 %, 30.41 % and 22.35 % respectively.

[DOI: 10.22068/ase.2022.598]

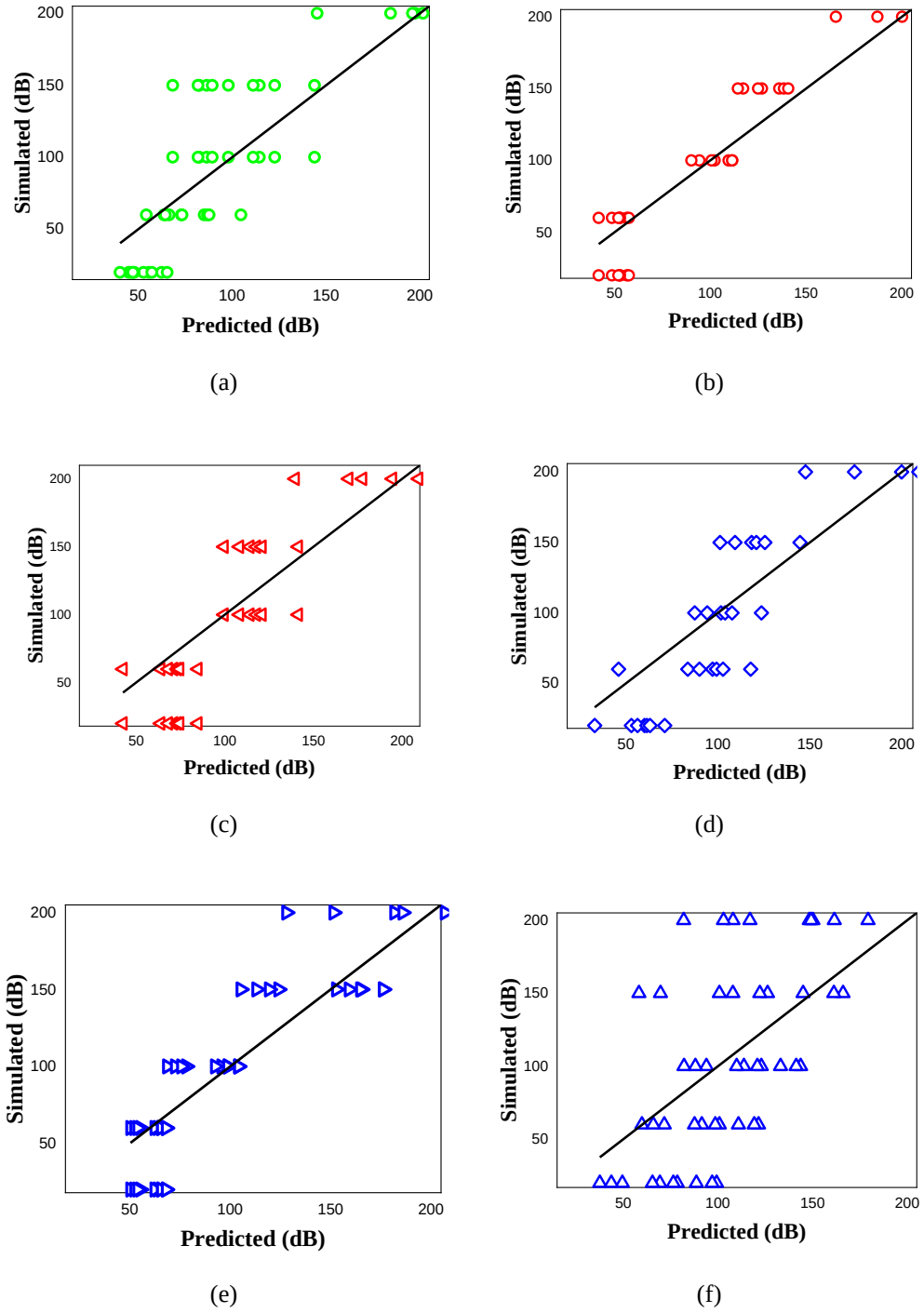

Figure 3 *Scatter Plots of Statistical Modeling (a) Kenaf Fibre (b) Polyester Fibre (c) Rockwool (d) Ceramic (e) Aerogel and (f) No liner*

The PLSR analysis further showed that even though Kenaf fibre had very good transmission Loss characteristics spanning over the entire frequency range, Aerogel, Rockwool, Ceramic, and Polyester had better prediction accuracy considering the number of peaks appearing in the transmission loss within the contour profile (Figure 2). Therefore, the higher the number of peaks the better the prediction accuracy.

4. Conclusion

In this paper, the performance of absorptive material liners on the transmission loss for farm products carrying tricycles has been evaluated using the finite element method and computational fluid dynamics. Literature has shown that the greater the ratio of packing surface area to flow area, the greater the attenuation capability of the muffler. The analysis has shown clearly that there

[DOI: 10.22068/ase.2022.598]

was a high correlation between the flow resistivity, temperature and mean fibre diameter. The results have also confirmed that absorptive material liners had effect on the transmission loss within medium to high frequency range. There was an obvious increase in the transmission loss to major peaks at different frequencies for all the absorptive material liners except for the Aerogel where several peaks occurred along the transmission path. The flow resistivity values for the absorptive materials used was inversely proportional to the transmission loss except the Kenaf fibre which had the highest transmission loss though with a second highest flow resistivity value. It has been observed that, the kenaf fibre, polyester, ceramic and rockwool performed well and showed good maximum transmission loss peaks. However, Kenaf fibre performed much better than the other absorptive material liners with a maximum transmission loss peak of 300 dB. In summary, the transmission loss for the muffler with absorptive material liners performed better than the muffler without an absorptive material liner [27, 28]. Research on noise levels relating to tricycles have shown that noise level increases with increasing load and speed regardless on the nature of the road [29, 30]. The transmission loss results obtained for the absorptive material liners Kenaf fibre, Ceramic, Polyester and Rockwool are better than the recorded noise levels. Therefore, introducing absorptive material liners in mufflers, optimizes the performance. Based on the results obtained for the CFD analysis the authors can propose that for effective noise control the optimum position for the absorptive material liner should be internal. This is because the flow has the best interaction with the absorptive material liner which improves the transmission loss. Subsequently, the authors recommend that kenaf fibre and polyester should be used for noise control in goods carrying tricycles because the performance.

References

1. Onwualu, A. and I. Olife, *Towards a sustainable value chain approach to agricultural transformation in Nigeria: the imperative of endogenous agricultural machinery development.* Journal of Agricultural Engineering and Technology, 2013. **21**(1): p. 1-17.
2. ElDidi, H., T.D. Bidoli, and C. Ringler, *Agriculture and youth in Nigeria: Aspirations, challenges, constraints, and resilience*. 2020.
3. Janardan, B., et al., *AST critical propulsion and noise reduction technologies for future commercial subsonic engines: separate-flow exhaust system noise reduction concept evaluation.* 2000.
4. Seo, S.-H. and Y.-H. Kim, *Silencer design by using array resonators for low-frequency band noise reduction.* The Journal of the Acoustical Society of America, 2005. **118**(4): p. 2332-2338.
5. Wang, B., et al. *Acoustic modelling and analysis of vehicle interior noise based on numerical calculation*. in *2010 International Conference on Intelligent Computation Technology and Automation*. 2010. IEEE.
6. Al-Zubi, M., et al., *Vibro-acoustic characterization and optimization of periodic cellular material structures (PCMS) for NVH applications.* Journal of Materials Science Research, 2013. **2**(4): p. 64.
7. Berardi, U. and G. Iannace, *Acoustic characterization of natural fibers for sound absorption applications.* Building and Environment, 2015. **94**: p. 840-852.
8. Fouladi, M.H., M. Ayub, and M.J.M. Nor, *Analysis of coir fiber acoustical characteristics.* Applied Acoustics, 2011. **72**(1): p. 35-42.
9. Wu, T., C. Cheng, and P. Zhang, *A direct mixed-body boundary element method for packed silencers.* The Journal of the Acoustical Society of America, 2002. **111**(6): p. 2566-2572.
10. George, T.C. and H.V. Raj. *Energy Efficient Design and Modification of an Automotive Exhaust Muffler for Optimum Noise, Transmission loss, Insertion loss and Back pressure: A Review*. in *IOP Conference Series: Materials Science and Engineering*. 2018. IOP Publishing Ltd.
11. Fu, J., et al., *Muffler structure improvement based on acoustic finite element analysis.* Journal of Low Frequency Noise, Vibration and Active Control, 2019. **38**(2): p. 415-426.
12. Verma, A. and M. Munjal, *Flow-acoustic analysis of the perforated-baffle three-chamber hybrid muffler configurations.* SAE International Journal of Passenger Cars-Mechanical Systems, 2015. **8**(2015-26-0131): p. 370-381.
13. Ebrahimi-Nejad, S. and M. Kheybari, *Honeycomb locally resonant absorbing acoustic metamaterials with stop band*

[DOI: 10.22068/ase.2022.598]

behavior. Materials Research Express, 2018. **5**(10): p. 105801.
14. Ebrahimi-Nejad, S. and M. Kheybari, *Composite Locally Resonating Stop Band Acoustic Metamaterials.* Acta Acustica united with Acustica, 2019. **105**(2): p. 313-325.
15. Kheybari, M. and S. Ebrahimi-Nejad, *Locally resonant stop band acoustic metamaterial muffler with tuned resonance frequency range.* Materials Research Express, 2018. **6**(2): p. 025802.
16. Arenas, J.P. and M.J. Crocker, *Recent trends in porous sound-absorbing materials.* Sound & vibration, 2010. **44**(7): p. 12-18.
17. Das, S., et al., *A novel design for muffler chambers by incorporating baffle plate.* Applied Acoustics, 2022. **197**: p. 108888.
18. Ferziger, J.H., M. Perić, and R.L. Street, *Computational methods for fluid dynamics*. Vol. 3. 2002: Springer.
19. Zhu, X., et al., *Recent advances in the sound insulation properties of bio-based materials.* BioResources, 2014. **9**(1): p. 1764-1786.
20. Vasile, O. and G.-R. Gillich, *Finite Element Analysis of Acoustic Pressure Levels and Transmission Loss of a Muffler*. Advances in Remote Sensing, Finite Differences and Information Security, 2012: p. 43-48.
21. Raj, M., S. Fatima, and N. Tandon, *A study of areca nut leaf sheath fibers as a green sound-absorbing material.* Applied Acoustics, 2020. **169**: p. 107490.
22. Alfonsi, G., *Reynolds-averaged Navier–Stokes equations for turbulence modeling.* Applied Mechanics Reviews, 2009. **62**(4).
23. EVRI, M., T. AKIYAMA, and K. KAWAMURA, *Coupling hyperspectral data with principle component regression (PCR) and partial least square regression (PLSR) to improve prediction accuracy of rice crop variables.* Journal of the Japanese Agricultural Systems Society, 2008. **24**(1): p. 31-42.
24. Gomez, T., et al., *Fique fibres as a sustainable material for thermoacoustic conditioning.* Applied Acoustics, 2020. **164**: p. 107240.
25. Lim, Z., et al., *Sound absorption performance of natural kenaf fibres.* Applied Acoustics, 2018. **130**: p. 107-114.
26. Asante, E.A., et al., *Detection and assessment of nitrogen effect on cold tolerance for tea by hyperspectral reflectance with PLSR, PCR, and LM models.* Information Processing in Agriculture, 2020.
27. Patne, M.M., S. Senthilkumar, and M.J. Stanley. *Numerical Analysis on Improving Transmission Loss of Reactive Muffler using Various Sound Absorptive Materials*. in *IOP Conference Series: Materials Science and Engineering*. 2020. IOP Publishing.
28. Ranjbar, M. and M. Alinaghi, *Effect of liner layer properties on noise transmission loss in absorptive mufflers.* Mathematical Modelling and Applications, 2016. **1**(2): p. 46-54.
29. Mondal, N.K., *Vehicle noise interference and its impact on the community.* Int J Curr Sci, 2013. **5**: p. 161-9.
30. Vergel, K.N., F.T. Cacho, and C.L.E. Capiz, *A Study on Roadside Noise Generated by Tricycles.* Philippine Engineering Journal, 2004. **25**(2).

[DOI: 10.22068/ase.2022.598]